Supporting Information

A Multifrequency Electron Spin Resonance Study of the Dynamics of Spin Labeled T4 Lysozyme

Ziwei Zhang[1], Mark R. Fleissner[2], Dmitriy S. Tipikin[1], Zhichun Liang[1], Jozef K. Moscicki[1,3], Keith A. Earle[1,4], Wayne L. Hubbell[2], Jack H. Freed[1*]

1. Department of Chemistry and Chemical Biology, Cornell University, Ithaca, NY 14853

2. Jules Stein Eye Institute and the Department of Chemistry and Biochemistry, University of California, Los Angeles, CA 90024

3. Smoluchowski Institute of Physics, Jagiellonian University, Reymonta 4, PL-30-059 Krakow, Poland

4. Department of Physics, University of Albany, SUNY, Albany, NY 12222

* Corresponding Author

Contents

Fitting procedure for determining magnetic tensor components

As noted in the Introduction, the 9 GHz spectra are more sensitive to the ***A*** tensor components, whereas the ***g*** tensor components can be accurately determined from the 170 GHz fits. An exception is A_{zz} which can be well estimated from spectral fits at both frequencies. The fitting process applied to the spectra of all four mutants is described as follows. First, the magnetic field (B_o^{zz}), corresponding to the central g_{zz} component in the spectrum, was measured directly at 170 GHz, based upon comparison of a standard sample of PD-Tempone in glycerol/water[1]. Then g_{zz} was calculated from $g_{zz} = \frac{h\nu}{\beta_e B_o^{zz}}$ with ν = 171.100 GHz. This value of g_{zz} was used in the following procedures. Then, the experimental 170 GHz spectra were fit by varying g_{xx}, g_{yy}, the ***A*** tensor and the Lorentzian inhomogeneous broadening (***W***) tensor. (Gaussian broadening was set to zero to simplify the fitting process.) The corresponding experimental 9 GHz spectrum was fit with g_{xx} and g_{yy} fixed at the values found from the 170 GHz fit, by varying the ***A*** tensor and the ***W*** tensor. Small uncertainties in ***g*** tensor parameters from the fits at 170 GHz have insignificant effect on the analysis of spectra at 9 GHz. Finally, the experimental 170 GHz spectrum was fit again by varying g_{xx}, g_{yy} and the ***W*** tensor with the ***A*** tensor components fixed at the values found from the 9 GHz fit. Magnetic tensor parameters listed in Table 2 are ***A*** tensor components from the 9 GHz fits and ***g*** tensor components from the 170 GHz fits. Values of A_{zz} found from the 170 GHz fits were identical (to within experimental and fitting certainties) to the ones from the 9 GHz fits.

Details on global nonlinear least squares (NLLS) fitting

In the fitting program, most of the fitting parameters are obtained from the global NLLS fits to the series of spectra obtained at multiple frequencies. The fitting parameters are varied until the sum of the differences between the best fits and the experiments at the various frequencies is minimized. The quality of the global fits is estimated by the reduced χ^2, which is calculated by[2]: $\chi^2 = \frac{1}{N_{total} - N_{parameter}} \sum_{j=1}^{N_{frequency}} \sum_{i=1}^{N_{data}} \left[\frac{(data_i - simulation_i)^2}{\sigma^2} \right]_j$ where N_{total} is the total number of data points of all frequencies, $N_{parameter}$ is the total number of fitting parameters. In this equation, σ is the standard deviation of the spectral noise, which is assumed to be constant throughout a spectrum but can be different for spectra at the different frequencies[3]. σ is obtained from the variance of a linear fit to the two baseline segments at either end of the spectrum that comprise 4%, 6%, 8% or 6% of the sweep width respectively of the spectrum obtained at 9, 95, 170 or 240 GHz[3]. In a global NLLS fitting, it is desirable that contributions to the reduced χ^2 from the spectral fits at each frequency should be weighted equally. For this purpose, first, a preliminary fitting to the multifrequency spectra was performed and the experimental data set was fit approximately with a set of fitting parameters. Then, some normally distributed noise was added at either end of the spectrum to adjust σ, so that the contributions to the reduced χ^2 from the preliminary fits at all frequencies are the same, before the final fitting. This guarantees that the spectra for the different frequencies are equally weighted in the fitting.

Unlike other fitting parameters, the relative population of each component in the multi-component fitting is a parameter sought by linear least-squares (LLS), and thus, cannot be preset to an initial value, but is determined at each iterative stage[3]. Generally, the population of a given component from the global fits to the multifrequency dataset is within 5% from the average population of this component from a group of single-frequency fits.

Supplement Table 1. Best fit parameters of nitroxide labeled T4 lysozyme in water solution [a]

mutant	T (°C)	comp.	$R^{o}_{\perp}$ (10^7 s^{-1})	$R^{o}_{\parallel}$ (10^7 s^{-1})	c_{20}	c_{22}	S_{20}	S_{22}	Popu.	R^{c} (10^7 s^{-1})	W_9 (G)	W_{95} (G)	W_{170} (G)	W_{240} (G)
72 R1	2	1	3.98	2.88	3.30	0.05	0.64	0.00	0.32	0.68	0.73	1.02	1.92	1.47
		2	40.7	0.16	3.49	-1.86	0.59	-0.16	0.38					
		3	49.0	0.42	3.21	-2.73	0.43	-0.31	0.30					
	12	1	5.62	3.47	3.30	0.18	0.64	0.01	0.22	1.00	0.76	1.50	1.30	1.56
		2	44.7	0.20	3.37	-1.75	0.58	-0.15	0.44					
		3	57.5	0.50	2.79	-1.98	0.45	-0.25	0.34					
	22	1	7.08	4.07	3.22	0.25	0.63	0.02	0.09	1.29	0.75	1.38	1.12	1.25
		2	49.0	0.19	3.31	-1.67	0.58	-0.15	0.48					
		3	63.1	0.63	2.62	-1.66	0.45	-0.22	0.43					
	32	2	57.5	0.22	3.24	-1.66	0.57	-0.16	0.50	1.62	0.79	1.32	1.94	0.88
		3	67.6	0.79	2.30	-1.30	0.43	-0.20	0.50					
131 R1	2	1	3.47	5.01	3.00	-0.16	0.60	-0.02	0.16	0.81	0.92	2.52	3.29	3.89
		2	47.9	1.66	2.85	-1.64	0.50	-0.19	0.54					
		3	37.2	0.63	1.31	1.34	0.20	0.32	0.30					
	12	1	4.07	5.89	3.00	-0.11	0.60	-0.01	0.14	1.29	0.86	2.16	2.61	2.37
		2	52.5	2.34	2.56	-1.55	0.45	-0.21	0.59					
		3	43.7	0.98	1.28	1.14	0.21	0.28	0.27					
	22	1	4.79	5.01	2.85	-0.03	0.58	0.00	0.06	1.51	0.79	1.82	3.87	1.94
		2	58.9	1.74	2.37	-1.23	0.45	-0.18	0.64					
		3	56.2	0.85	1.29	0.79	0.25	0.19	0.30					
	32	2	63.1	2.40	2.21	-0.98	0.44	-0.15	0.61	1.91	0.81	2.30	3.99	4.87
		3	60.3	1.07	1.24	0.77	0.24	0.19	0.39					
72 R2	2	1	4.27	3.89	3.41	-0.09	0.65	-0.01	0.73	0.69	0.60	0.19	1.88	
		2	33.1	2.14	2.91	-0.87	0.57	-0.09	0.27					
	12	1	5.62	5.13	3.40	-0.08	0.65	-0.01	0.61	1.02	0.57	1.11	1.67	
		2	39.8	2.51	2.94	-0.66	0.58	-0.07	0.39					
	22	1	8.71	6.03	3.40	0.02	0.65	0.00	0.51	1.29	0.60	0.34	1.30	
		2	46.8	4.57	2.96	-0.79	0.58	-0.08	0.49					
	32	1	11.7	8.13	3.30	-0.27	0.64	-0.02	0.45	1.78	0.55	0.36	0.93	
		2	51.3	6.03	2.91	-0.64	0.58	-0.07	0.55					
131 R2	2	1	9.12	1.66	3.73	-0.74	0.68	-0.05	0.56	0.68	0.76	1.55	3.22	3.67
		2	42.7	3.02	2.81	0.43	0.57	0.05	0.44					
	12	1	11.0	1.86	3.70	-0.91	0.67	-0.06	0.44	0.98	0.68	1.49	2.38	3.95
		2	50.1	3.89	2.80	0.44	0.57	0.05	0.56					
	22	1	12.9	2.45	3.65	-1.23	0.65	-0.09	0.37	1.23	0.68	1.67	1.96	3.77
		2	60.3	6.31	2.75	0.51	0.56	0.06	0.63					
	32	1	15.8	6.76	3.60	-0.76	0.66	-0.05	0.35	1.78	0.58	1.17	2.98	3.30
		2	69.2	7.41	2.75	0.77	0.55	0.09	0.65					

[a] Estimated errors: $R^{o}_{\perp} \leq 7\%$, $R^{o}_{\parallel} \leq 17\%$; $c_{20} \leq 5\%$; $S_{20} \leq (\pm 0.02)$, $S_{22} \leq (\pm 0.05)$; Popu $\leq (\pm 0.05)$; $R^{c} \leq 7\%$.

Supplement Table 2. Best fit parameters of nitroxide labeled T4 lysozyme in 15 and 25 w/v% Ficoll solutions [a]

mutant	T (°C)	comp.	$R^{o}_{\perp}$ (10^7 s^{-1})	$R^{o}_{\parallel}$ (10^7 s^{-1})	c_{20}	c_{22}	S_{20}	S_{22}	Popu.	R^{e} (10^7 s^{-1})	W_9 (G)	W_{95} (G)	W_{170} (G)	W_{240} (G)
131 R1 in 25% Ficoll	2	1	3.55	2.00	3.10	-0.02	0.62	0.00	0.24	0.12	1.14			2.79
		2	46.8	0.69	2.80	-1.42	0.51	-0.17	0.52					
		3	37.2	0.63	1.10	-0.35	0.24	-0.09	0.24					
	12	1	4.47	1.91	3.03	0.07	0.61	0.01	0.17	0.23	1.02			4.26
		2	50.1	0.79	2.72	-1.46	0.49	-0.18	0.60					
		3	49.0	0.79	1.08	-0.07	0.24	-0.02	0.23					
	22	1	4.68	1.78	2.87	-0.07	0.59	-0.01	0.10	0.41	0.87			4.37
		2	51.3	1.55	2.63	-1.38	0.48	-0.18	0.57					
		3	46.8	0.79	1.20	0.04	0.27	0.01	0.33					
	32	2	58.9	2.51	2.56	-1.52	0.46	-0.21	0.71	0.60	0.85			4.52
		3	60.3	1.00	1.20	0.81	0.23	0.21	0.29					
72 R2 in 15% Ficoll	2	1	2.69	2.82	3.43	-0.32	0.66	-0.02	0.65	0.17	0.70	0.56	1.46	
		2	33.9	2.04	3.29	-1.03	0.62	-0.09	0.35					
	12	1	4.07	3.80	3.42	-0.28	0.65	-0.02	0.62	0.35	0.62	0.46	1.85	
		2	40.7	2.40	3.13	-0.85	0.60	-0.08	0.38					
	22	1	6.03	4.90	3.41	-0.07	0.65	-0.01	0.48	0.63	0.64	0.75	1.73	
		2	45.7	3.31	3.10	-0.77	0.60	-0.07	0.52					
	32	1	8.32	6.31	3.30	-0.39	0.64	-0.03	0.40	0.91	0.57	1.09	1.38	
		2	51.3	5.01	3.03	-0.61	0.60	-0.06	0.60					
72 R2 in 25% Ficoll	2	1	1.91	2.24	3.49	-0.62	0.66	-0.05	0.65	0.10	0.63	0.67	1.79	
		2	33.9	1.66	3.35	-1.17	0.62	-0.10	0.35					
	12	1	2.75	2.75	3.45	-0.43	0.66	-0.03	0.58	0.20	0.65	0.91	1.94	
		2	38.0	2.82	3.31	-1.01	0.62	-0.09	0.42					
	22	1	3.98	3.89	3.40	0.06	0.65	0.01	0.50	0.38	0.63	0.97	2.08	
		2	44.7	2.82	3.30	-1.00	0.62	-0.08	0.50					
	32	1	5.50	4.37	3.30	-0.50	0.64	-0.04	0.39	0.50	0.61	1.24	2.08	
		2	51.3	5.37	3.19	-0.60	0.62	-0.05	0.61					
131 R2 in 15% Ficoll	2	1	6.03	1.35	3.74	-0.69	0.68	-0.04	0.63	0.21	0.75	1.13	3.70	
		2	42.7	7.08	2.97	0.33	0.60	0.03	0.37					
	12	1	7.08	1.62	3.72	-0.62	0.68	-0.04	0.49	0.43	0.70	1.03	3.59	
		2	46.8	3.89	2.80	0.11	0.58	0.01	0.51					
	22	1	10.0	1.70	3.66	-1.16	0.66	-0.08	0.44	0.65	0.63	1.65	2.75	
		2	58.9	4.37	2.77	0.36	0.57	0.04	0.56					
	32	1	12.9	2.19	3.64	-1.27	0.65	-0.09	0.40	1.00	0.55	1.50	2.53	
		2	69.2	7.41	3.01	0.93	0.58	0.09	0.60					
131 R2	2	1	4.07	1.07	3.75	-0.77	0.68	-0.05	0.65	0.11	0.83	1.28	3.36	3.71
		2	41.7	3.02	2.98	0.31	0.60	0.03	0.35					
	12	1	4.57	1.70	3.70	-1.19	0.66	-0.08	0.49	0.21	0.79	1.40	2.79	3.56

in 25% Ficoll		2	50.1	2.88	2.84	-0.05	0.58	-0.01	0.51					
	22	1	5.37	1.66	3.68	-1.07	0.66	-0.07	0.46	0.42	0.63	1.36	3.01	3.91
		2	58.9	2.51	2.82	-0.01	0.58	0.00	0.54					
	32	1	6.61	2.19	3.68	-1.78	0.62	-0.13	0.40	0.58	0.54	1.48	2.55	4.39
		2	67.6	3.47	2.86	0.33	0.58	0.04	0.60					

[a] Estimated errors: Same as in Supplement Table 1.

Two vs. three component fits to spectra of 131R1

For 131R1, the spectral features corresponding to an immobile component can be observed in the high field spectra of 131R1 but cannot be resolved in the 9 GHz spectrum in aqueous solution (see Supplement Figure **1A**). (However, in viscous solution, it is possible to see the immobile component even at 9 GHz[4].) We tried to simulate the spectra of 131R1 at 2°C with two components: an immobile component and a relatively mobile component. Similar to the two component fitting for 72R1, two small outer peaks are present in the simulated 9 GHz spectrum but not in the experimental data (see Supplement Figure **1B**), and the g_{zz} region of the 240 GHz spectrum cannot be well fit (see Supplement Figure **1B**). Moreover, the spectral features in the central region of the 95 GHz spectrum cannot be reproduced (see Supplement Figure **1B**). Consequently, a third component was found to be necessary to reproduce the spectral features at all frequencies. This third component corresponds to the most mobile component amongst the three; (see Supplement Figure **1C** showing this component in the 95 GHz simulation). It also led to the same populations of the components for all four frequencies.

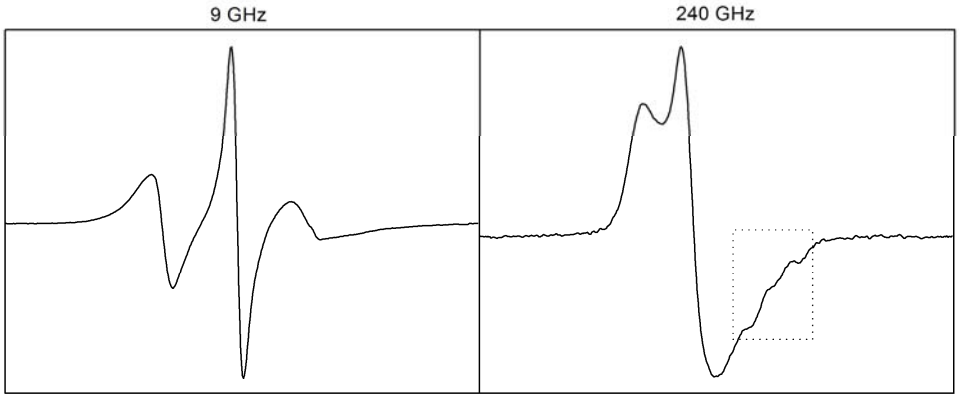

Supplement Fig. 1A. The 9 and 240 GHz experimental data of 131R1 recorded at 2 °C. The dashed rectangle shows the immobile component features that can be observed by eye in the 240 GHz spectrum, but not in the 9 GHz spectrum.

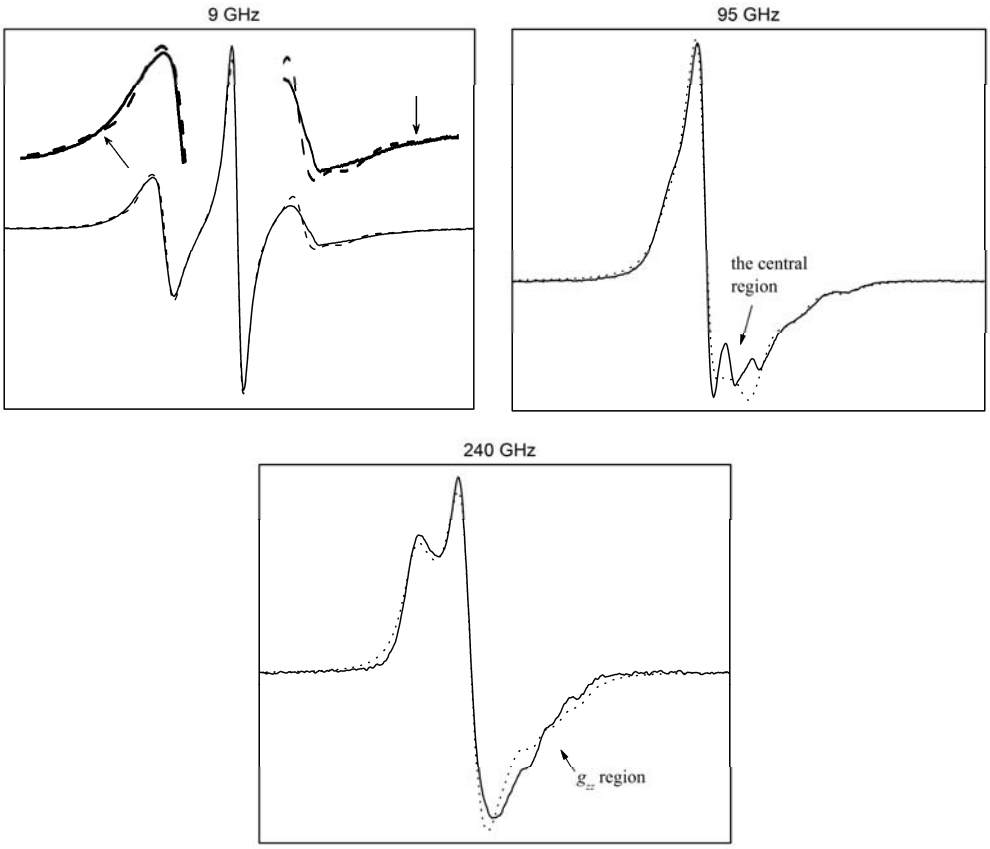

Supplement Fig. 1B. The two component fits to the 9, 95 and 240 GHz spectra of 131R1 recorded at 2 ^{o}C; experimental data (solid lines), simulations (dashed lines). The arrows respectively point to the two outer peaks present in the two component fit but not in the experimental data at 9 GHz, the poor fit to the central region of the 95 GHz spectrum, and the poor fit to the g_{zz} region of the 240 GHz spectrum.

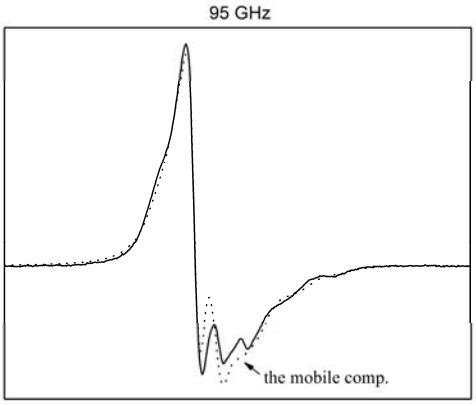

Supplement Fig. 1C. The three component fit to the 95 GHz spectrum of 131R1 recorded at 2 ^{o}C; experimental data (solid line), simulation (dashed line). The fit to the central region is improved by the addition of the third component (i.e. the mobile component).

Single-component fits to spectra of 72R2

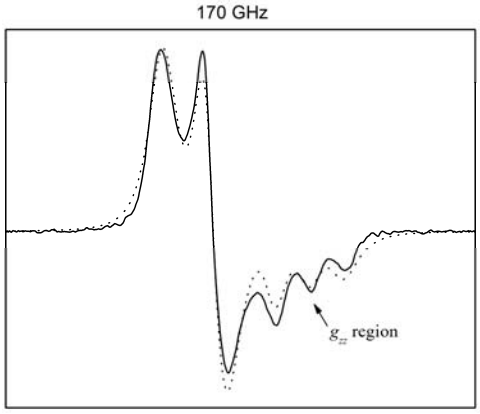

Supplement Fig. 2. The single component fit to the 170 GHz spectrum of 72R2 recorded at 2 ^{o}C; experimental data (solid line), simulation (dashed line). The arrow points to the g_{zz} region that is not well fit.

Single-component fits to spectra of 131R2

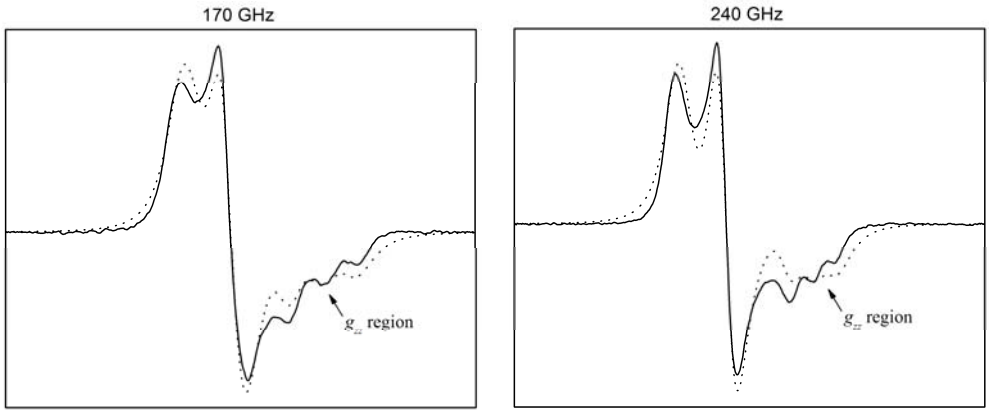

Supplement Fig. 3. The single component fits to the 170 and 240 GHz spectra of 131R2 recorded at 2 ^{o}C; experimental data (solid lines), simulations (dashed lines). The arrow points to the g_{zz} region that is not well fit.

Variation of the reduced χ^2 with the diffusion tilt angle (β_d)

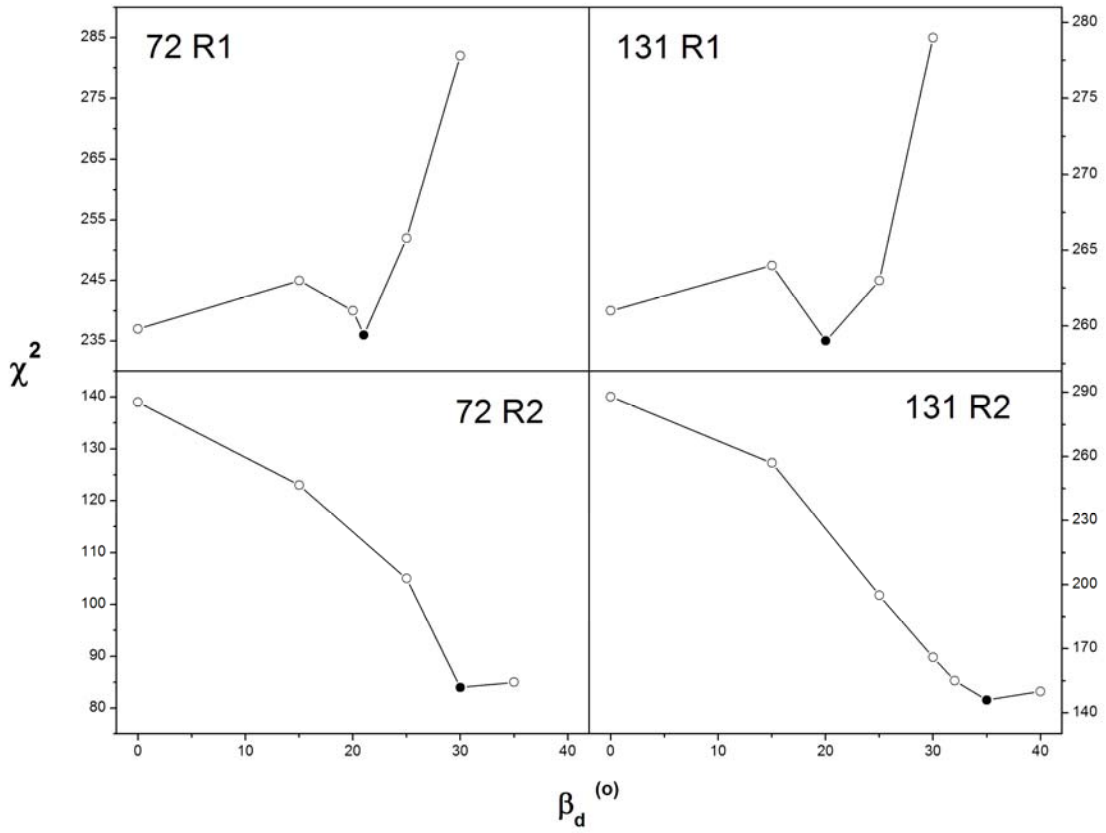

Supplement Fig. 4. The reduced χ^2 from the best fits to the multifrequency spectra recorded at 2 ^{o}C in water solution vs the diffusion tilt angle (β_d); the best fit β_d (●).

Further discussion of spectra recorded in 65 w/w% sucrose solution

In the previous study on 72R1 and 131R1, it was assumed that 65 w/w% sucrose solutions provided virtually rigid-limit spectra[2]. Our study encompassing the range of -50°C to +10°C clearly demonstrates that at +10°C the spectra are significantly affected by motion. Thus the true rigid-limit *g* and *A* tensors given in Table 2 show some differences with those reported in the previous study. But a comparison of the estimates of these tensors from our current +10°C spectra, when incorrectly interpreted as rigid limit spectra, yields relative results in rather good agreement with those reported previously. The most prominent effects of the increase in temperature are an apparent substantial increase in g_{zz}, a decrease in g_{xx}, and a very small decrease in g_{yy}. [Also, A_{zz} appears to decrease, while A_{yy} increases, but A_{xx} hardly changes]. The differences previously noted in the magnetic tensors for 72R1 and 131R1 at +10°C were tentatively ascribed to local polarity differences[2]. Our present study makes clear that the true rigid-limit magnetic tensors in 65% sucrose are identical, and the differences at +10°C result from differences in their mobilities.

At 10°C, the identical spectra observed for 72R2 and 131R2 can be fit as rigid limit spectra by varying magnetic and linewidth tensors, but these variations as well as their broader lines than for -50°C spectra indicate incipient slow motion. They can be fit with just a single component, i.e. the immobile component. The absence of the intermediate component could suggest that the equilibrium has substantially shifted to the immobile component in 65% sucrose solution vs. aqueous solution or else the near rigid spectra provide much too limited features to discriminate two components.

In the spectra of R2 from -50 to 10°C, the deviations of magnetic tensors from the rigid limit ones are caused by the residual diffusion of the spin label. We made two assumptions for how the diffusion of the spin label varies with

temperature: (1) R^o increases with increasing temperature; and (2) S_{20} decreases with increasing temperature. For assumption (1), we performed some simulations with the full range of axial and non-axial symmetries for the R^o tensor. For assumption (2), we performed some simulations with *x*-, *y*-, and *z*-ordering. By comparing the change of the ***g*** tensor in the simulated 170 GHz spectrum and A_{zz} in the simulated 9 GHz spectrum with the change of these tensor components in the experimental spectra, we reached the following conclusions respectively for the two assumptions: (1) $R^o_{\parallel}$ cannot be greater than $R^o_{\perp}$; and (2) the *z*-ordering model is much better than the *x*- and *y*-ordering models. These observations are consistent with our results in water and Ficoll solutions which show that: (1) $R^o_{\parallel}$ is typically much smaller than $R^o_{\perp}$; and (2) the internal diffusion of the spin label shows *z*-ordering.

The spectra of 72R1 and 131R1 in 65% sucrose at 10°C are clearly slow motional, but these spectra cannot be well fit with a single component. This further supports that, at 10°C, there should be at least a second component for R1. One component is an immobile one, and the other is a relatively mobile one. Qualitatively, the simulations show that the population for the immobile component is ~65%, vs. ~20% in water solution, suggesting that the equilibrium shifts to the immobile component in 65% sucrose. Some amount (~35%) of the intermediate and/or the mobile component still exists, and the difference in their motilities at site 72 and site 131 makes the spectra of 72R1 and 131R1 different at 10°C in 65% sucrose solution. The equilibrium shift towards the immobile component in sucrose solution was also suggested by Guo by showing that 30% sucrose shifts the equilibrium towards the immobile component at some interacting surface sites of T4L[5].

Contribution of the global tumbling in 25% Ficoll solution

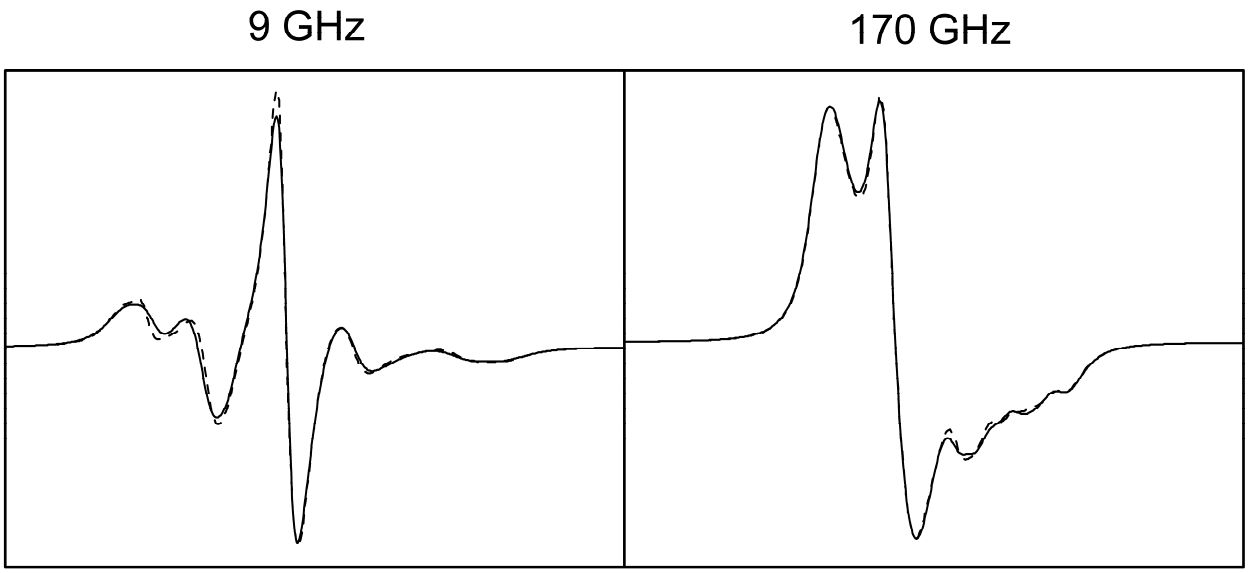

Supplement Fig. 5. Comparison of 9 and 170 GHz simulated spectra with the global tumbling rate (R^c) set to the value in 25 w/v% Ficoll solution (solid line) and to the rigid limit value, i.e. $3.2*10^5$ s^{-1}, (dashed line) respectively. All other parameters were the best fit ones for 72R2 at 22^{o}C in 25 w/v% Ficoll solution (see Supplement Table 2).

References

(1) Budil, D. E.; Earle, K. A.; Lynch, W. B.; Freed, J. H. Electron Paramagnetic Resonance at 1 millimeter Wavelengths. In *Advanced EPR: Applications in Biology and Biochemistry;* Hoff, A., Ed.; Elsevier: Amsterdam, 1989; Chapter 8, pp 307-340.

(2) Liang, Z.; Lou, Y.; Freed, J. H.; Columbus, L.; Hubbell, W. L. A Multifrequency Electron Spin Resonance Study of T4 Lysozyme Dynamics using the Slowly Relaxing Local Structure Model. *The Journal of Physical Chemistry B* **2004**, *108*, 17649-17659.

(3) Budil, D. E.; Lee, S.; Saxena, S.; Freed, J. H. Nonlinear-Least-Squares Analysis of Slow-Motion EPR Spectra in One and Two Dimensions using a Modified Levenberg-Marquardt Algorithm. *J. Magn. Reson. , Series A* **1996**, *120*, 155-189.

(4) Fleissner, M. R.; Cascio, D.; Hubbell, W. L. Structural Origin of Weakly Ordered Nitroxide Motion in Spin-Labeled Proteins. *Protein Sci.* **2009**, *18*, 893-908.

(5) Guo, Z. Ph.D. Thesis, University of California, Los Angeles, 2003.